

Basin entropy and the impact of the escape positioning in an open area-preserving map

P. Haerter¹, R.L. Viana², and M.A.F. Sanjuán³

¹Departamento de Física, Universidade Federal do Paraná, Curitiba, Paraná, Brazil

²Centro Interdisciplinar de Ciência, Tecnologia e Inovação, Núcleo de Modelagem e Computação Científica, Universidade Federal do Paraná, Curitiba, Paraná, Brazil

³Nonlinear Dynamics, Chaos, and Complex Systems Group, Departamento de Física, Universidad Rey Juan Carlos, Móstoles, Madrid, Spain

October 1, 2024

Abstract

The main properties of a dynamical system can be analyzed by examining the corresponding basins, either attraction basins in dissipative systems or escape basins in open Hamiltonian systems and area-preserving maps. In the latter case, the selection of the openings is crucial, as the way exits are chosen can directly influence the results. This study explores the impact of different opening choices on the escape basins by employing a model of particles transported along field lines in tokamaks with reversed shear. We quantitatively evaluate these phenomena using the concept of basin entropy across various system configurations. Our findings reveal that the positioning of the exits significantly affects the complexity and behavior of the escape basins, with remarkable abrupt changes in basin entropy linked to the choice of exits.

Keywords: **tokamak, reversed shear, escape basin, basin entropy, fractal basin boundary**

1 Introduction

A basin of attraction is defined as the set of points that, when taken as initial conditions, are drawn to a specific attractor. This concept is a fundamental tool for exploring dissipative dynamical systems [1,2]. When dealing with conservative Hamiltonian systems, the total energy is conserved, and thus, we cannot speak about attractors or basins of attraction. Nevertheless, while we cannot talk about attractors in these systems, we can open them, defining exit basins in an analogous way to the basins of attraction in a dissipative system.

An exit or escape basin represents the set of initial conditions that lead to a given exit, allowing trajectories to escape through it. These ideas regarding continuous dynamical systems can be extended to discrete dynamical systems, where area is preserved rather than energy,

leading to the classification of these systems as area-preserving maps. In some Hamiltonian systems, such as the Hénon-Heiles Hamiltonian, the system becomes open for energies above a certain threshold, commonly referred to as the escape energy. In this case, the potential opens up, revealing three natural exits through which an orbit may escape to infinity. However, in other conservative systems or area-preserving maps the opening may be implemented artificially, leading to different possible configurations. The placement of the escape region significantly influences the structure and properties of the escape basins [4–6].

A powerful tool for quantifying the complexity of basins, either basins of attraction or escape basins, is the notion of basin entropy [3], which measures the degree of mixing and unpredictability within the basin structure in phase space. Basin entropy, S_b , is computed by dividing the phase space into small regions and calculating the Shannon entropy of the escape dynamics within each region. The average entropy across the entire phase space yields an overall measure of the complexity of the escape basin. Additionally, focusing on the boundaries of the escape basins gives the basin boundary entropy, S_{bb} , which captures the intricate and often fractal nature of the basin boundaries, a hallmark of chaotic behavior.

This work focuses on understanding how the choice of the escape region impacts both the escape basin structures and the basin entropy, revealing how sensitive conservative systems are to the configuration of their escape mechanisms. We explore these questions using the Revtokamak model, an area-preserving map that represents the magnetic field lines within a toroidal confinement device used in plasma fusion experiments [7]. The motivation for studying this model comes from the need to understand the escape of high-energy particles from the plasma, which can damage the tokamak walls and disrupt confinement, posing challenges for plasma stability [8]. By introducing different escape regions in this model, we can study how particle trajectories leave the system and how the escape basins evolve under various conditions.

Previous studies employed a straightforward method to open the system by splitting the phase space at the center, without fully accounting for the system’s underlying dynamics [9]. This approach yielded surprising and unresolved results regarding both basin entropy and basin boundary entropy as system parameters were varied. These findings suggest that the choice of a particular escape region significantly impacts the system’s chaotic properties, especially in terms of how basin structures respond to perturbations.

In this paper, we aim to explore how different placements of escape regions affect the resulting escape basins and the corresponding entropic measures in the Revtokamak model. As a result, we have found that the escape orbits move in the anticlockwise direction when the perturbation of the system is increased. This movement can cause a discontinuity in the basins depending on the positioning of the escape regions, and this leads to an abrupt change in the basins that can be captured using entropic measures.

This paper is organized as follows. In Section 2, we introduce the Revtokamak model and its significance. Section 3 investigates how the positioning of escape regions influences both basin entropy and basin boundary entropy, while Section 4 summarizes the key findings and conclusions of this study.

2 The Revtokamap model

The Revtokamap [7, 10] represents a model of the magnetic field line in toroidally confined plasmas with the presence of reversed shears, and its mathematical formulation is given by

$$\begin{aligned}
r_{n+1} &= \frac{1}{2} \left\{ P(r_n, \theta_n) + \sqrt{[P(r_n, \theta_n)]^2 + 4r_n} \right\}, \\
\theta_{n+1} &= \theta_n + W(r_{n+1}) - \frac{K}{(2\pi)^2} \frac{r_{n+1} \cos(2\pi\theta_n)}{(1 + r_{n+1})^2},
\end{aligned} \tag{1}$$

where

$$P(r_n, \theta_n) = r_n - 1 - \frac{K}{2\pi} \sin(2\pi\theta_n), \tag{2}$$

$$W(r) = w[1 - a(cr - 1)^2], \tag{3}$$

allowing us to study the behavior of possibly chaotic orbits of particles attached to the field lines more simply than the direct use of the whole set of differential equations for the field lines.

This map represents the Poincaré section in a toroidal space, where the variable r describes the radial position between the center at $r = 0$ and the border at $r = 1$ of the device, and variable θ is the periodic coordinate of the field lines, that for this system is normalized between 0 and 1. The K parameter is the perturbation parameter, representing the external perturbations that can interfere in the experiment and causes the increase of chaoticity of the field lines. Since energy is conserved, our map should be an area-preserving map, and this implies that the value of the perturbation parameter should be defined in the range $K \in [0, 2\pi)$.

The main property of this map is the freedom to chose the W function, that represent the winding number profile inside the tokamak. To reduce the transport of the field lines and improve confinement, the W function is chosen to be a non-monotonic function, breaking the twist condition and inducing the presence of reversed shears. This allows the formation of transport barriers, providing a more interesting case for study in plasma physics [9, 11, 12].

3 Impact of the opening choice on the escape dynamics

To explore and analyze how the choice of the different ways of opening the system affects the dynamic properties of the escape, we divide the tokamak wall ($r = 1$) into equal segments with a different configuration. We will consider the following cases:

- **LR Case.** It was previously used in [9], and splits the phase space into two exits: $0 \leq \theta < 0.5$, labeled as L , and $0.5 \leq \theta \leq 1.0$, labeled as R .
- **BC Case.** Due to the periodicity of θ , it is possible to apply a 90° rotation in the basins, making one basin at the borders: $0 \leq \theta < 0.25 \cup 0.75 < \theta \leq 1.0$, labeled as B , and the other in the center: $0.25 \leq \theta \leq 0.75$, labeled as C .
- **Multi Case.** This division splits the phase space into ten different exits, providing a more granular analysis of the escape behavior.

Figure 1 illustrates how the different escape choices affects the way phase-space points are distributed in the basins, even though the perturbation value is kept constant between the figures. It is possible to see that for the LR case, there is a large mixture of blue and red points close to the quasi-periodic islands, with both colors intertwined.

When the exits are rotated 90° , the basins change substantially, with a predominance of the red basin over the blue one. The BC case shows that most of the particles escape, reaching the tokamak wall, along the symmetry axis. This part would receive more energy in real cases and

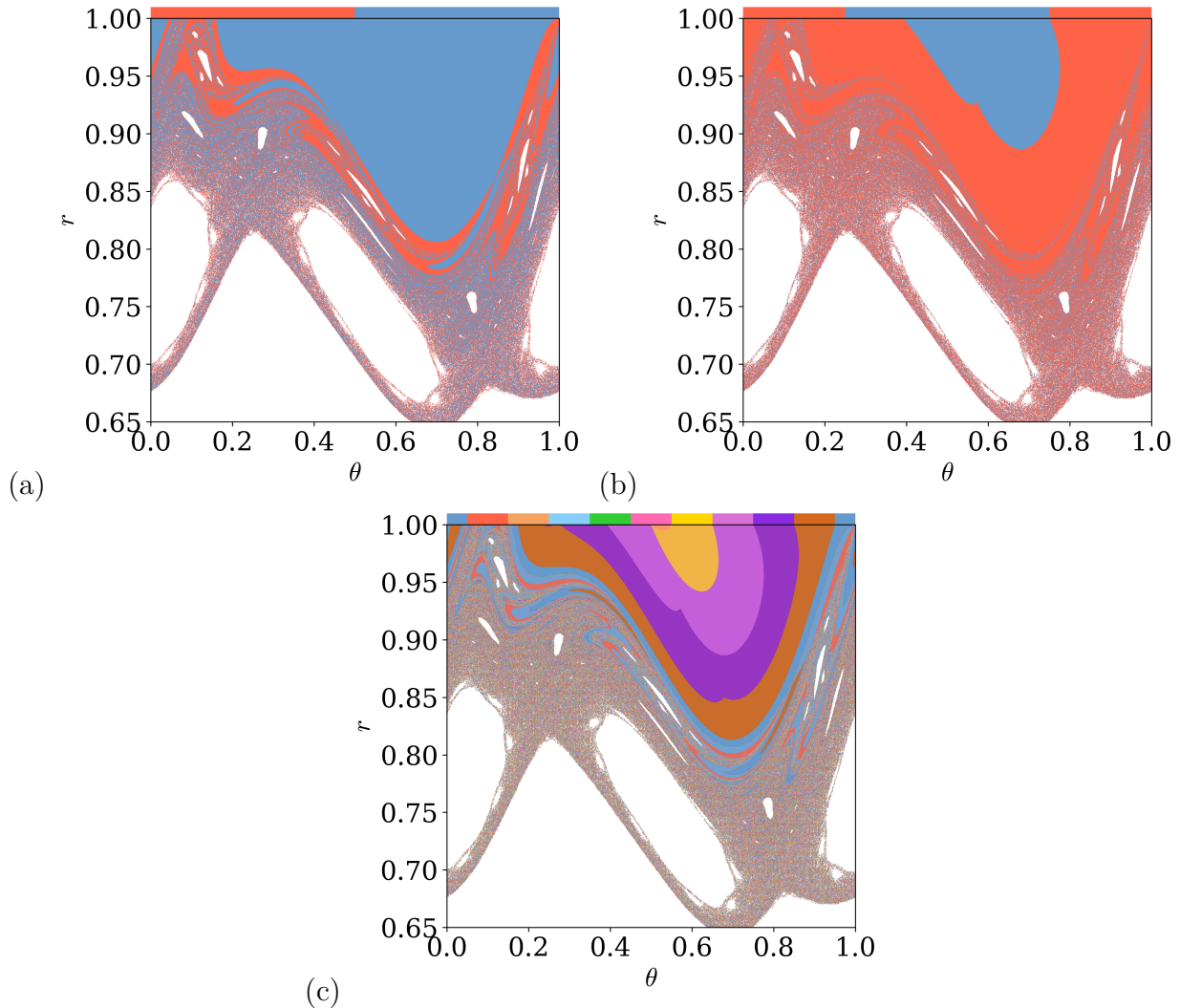


Figure 1: Escape basins for the Revtokamap with the same perturbation parameter $K = 2.1$, for the three cases presented: (a) *LR* with the *L* (red) and *R* (blue) exits, (b) *BC* with the *B* (red) and *C* (blue) exits, and (c) *Multi* case, with 10 different exits represented in the figure. The color on top of each plot represents the exit region for each color. The plots reveal how just changing the position and number of exits changes the escape basin and also show some preferable regions of escape for this perturbation value.

thus requires a higher protection. The central part receives some chaotic particles, but most of them come from the same regular region, marked by the blue spot.

With that in mind, the *Multi* case considers one basin in the symmetry axis and splits the other nine around it, allowing for a higher knowledge about where the particles escape. A visual analysis of Fig. 1 (c) shows a higher number of points in blue (exit in the symmetry axis) and the closer regions (in red and dark brown).

To quantify this mixture and how each choice of exits affects it, we use the basin entropy [3]. Covering all the escape regions with a finite number N of boxes of size ε and computing the corresponding escape probabilities, assuming they are equiprobable:

$$p_i = \frac{n_i}{\varepsilon^2}, \quad (4)$$

where $i \in [1, N_A]$ refers to each exit and N_A is the number of the exit. The Shannon entropy

for the i th cell is thus

$$S_i = - \sum_{i=1}^{N_A} p_i \log p_i. \quad (5)$$

Since this entropy is additive (extensive), the total entropy of the mesh will be the sum over all boxes, divided by their number:

$$S_b = \frac{1}{N} \sum_{i=1}^N S_i, \quad (6)$$

which is what we call basin entropy.

For boxes with just one attractor inside, the Shannon entropy will be zero. Discarding them in the calculation leads to another measure, the basin boundary entropy, where only boxes with more than one attractor inside are considered, and is defined as

$$S_{bb} = \frac{1}{N_b} \sum_{i=1}^N S_i, \quad (7)$$

where N_b represents the number of boxes with multiple attractors inside. This quantity is more sensitive to changes in the phase space and the presence of multiple attractors close to each other.

These two quantifiers can be used to analyze the mixture and uncertainty about the initial conditions in either a escape basin or a basin of attraction. When $S_b \rightarrow 0$, in a small box of ε^2 , almost all the initial conditions lead to the same exit, providing a higher knowledge about their sensitivity. When $S_b \rightarrow \ln N_a$, the distribution of points inside the box is almost equal, leading to a higher uncertainty in the initial conditions.

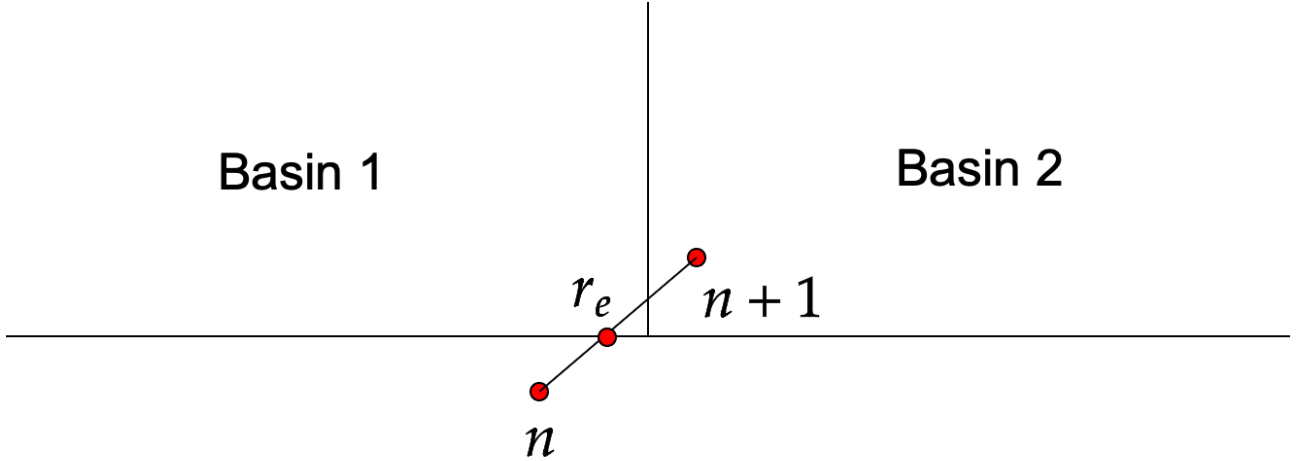


Figure 2: Representation of the escaping point and how the definition can influence the characterization of a basin. The points n and $n + 1$ represent two iterates of the map, showing the transition between regions. The point r_e represents the interpolation point calculated using the Eq. (8), indicating where the point should escape. This demonstrates that the point should be classified as from Basin 1 rather than Basin 2.

Instead of just considering the next point as the exit point, for this study, we consider a linear interpolation of the points to obtain a more accurate exit position, leading to a better classification of the basins. Figure 2 exemplifies how this change can influence the obtained results, and Eq. (8) shows how the points were interpolated

$$r_e = r_n + (r_{n+1} - r_n) \frac{1 - \theta_n}{\theta_{n+1} - \theta_n}. \quad (8)$$

Figure 3 represents the basin entropy and the basin boundary entropy, along with the fraction area of each basin for the three cases under study. The results observed for all cases show the expected increase in basin entropy with higher values of the perturbation parameter due to the increasing chaoticity of the system and the corresponding increase in fractality.

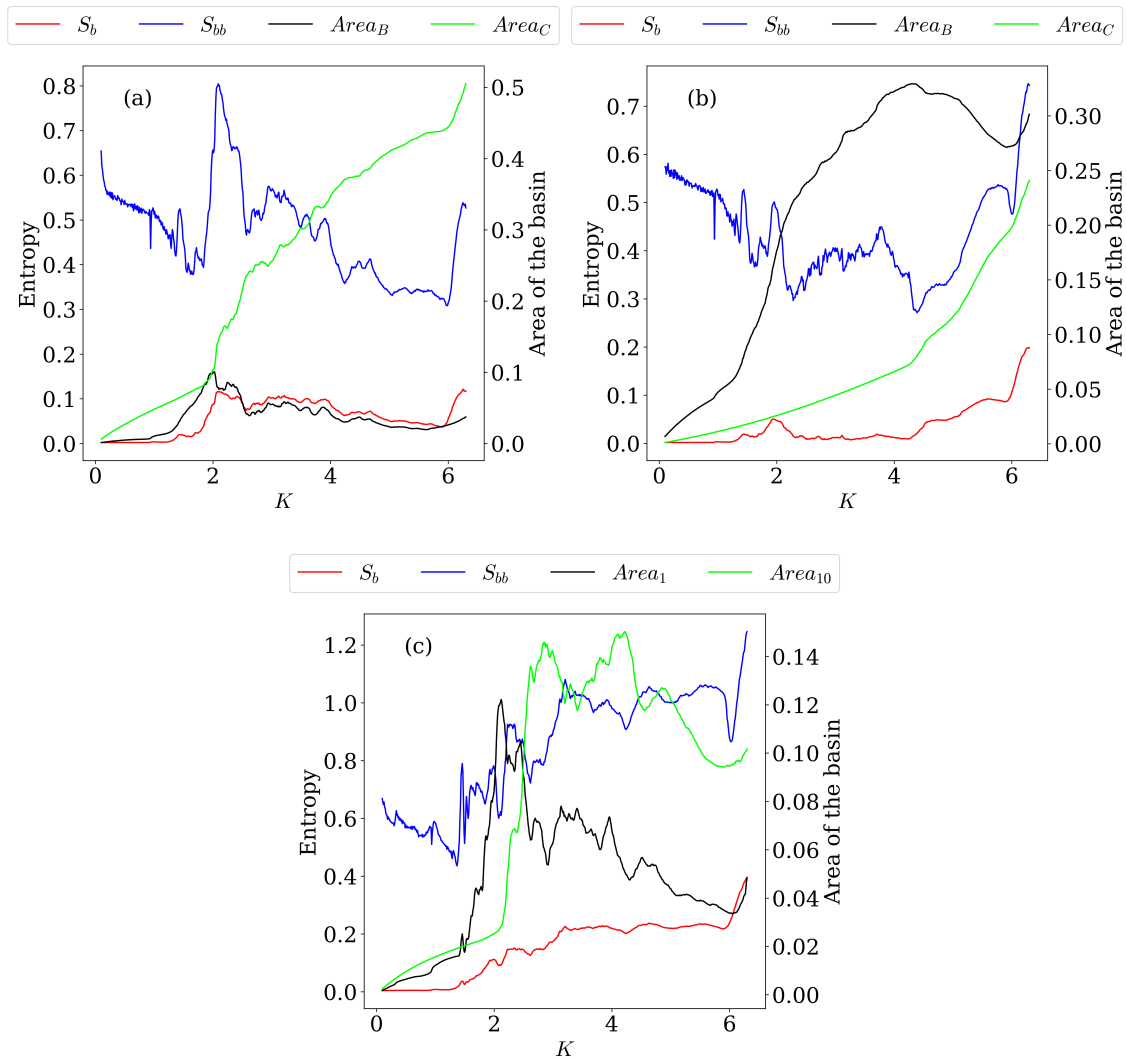


Figure 3: Basin entropy (black), basin boundary entropy (green), and basin area fraction of the basins as a function of the parameter K for the Revtokamap for the (a) *LR* case, (b) *BC* case, and (c) *Multi* case. The plot shows the relationship between these quantities, revealing how the basin entropy and the basin boundary entropy are influenced by the occupied areas and how these two quantities can change with the increase of the perturbation parameter.

One result that was left unexplained in [9] is why an abrupt change occurs in the basin entropy and the basin boundary entropy in the region of $K_c = K \approx 2$. We reproduced such

behavior in Fig. 3(a), where it is possible to see a continuous behavior for lower values of K_c , a big change in the basin entropy, and then the basin entropy starts to decrease. The difference in basin entropy and basin boundary entropy and areas compared to the original results arises from the more precise method for determining where particles escape.

Besides the difference caused by the interpolation, it is also possible to see in Fig. 3(a) that close to K_c , the area of the R basin increases abruptly. In contrast, the L basin area remains almost constant. This has a direct effect on S_b and S_{bb} , where the highest basin boundary entropy occurs when both areas are at their maximum values. The dominance of one exit over the other, even though the system exhibits more chaotic behavior due to the increase in the perturbation parameter, leads to a decrease in the basin entropy.

On the other hand, when the system is rotated, as represented in Fig. 1(b), the basin entropy remains close to zero for higher values of K , with the area of the red basin being dominant over the blue one, until a high perturbation value of $K \approx 4$ where the second one starts to increase and, with it, the basin entropy starts to rise. This type of behavior shows a preference for escape positions along the symmetry axis, which is changed only for high values of the perturbation K .

The *Multi* case provides more insight into this discussion. Due to the arbitrary choice of the exits, some preferences can be made, influencing how the results will be interpreted. By positioning one of the exits on the symmetry axis and expanding the number of exits, we can observe a more precise behavior of the basins and how they change with the perturbation parameter.

With Fig. 1(c), it is possible to see a relative tendency of the particles to move to the right, due to all the smooth regions being connected to the exits on the right side of the polar direction. Along with this, when analyzing the basin entropy and areas in Fig. 3(c), it is possible to observe a movement of the basin areas in the counterclockwise direction. For lower values of K , there is a higher escape in the first exit located in the region close to the symmetry axis. Upon reaching the value of $K \approx 2.5$, its value decreases, and simultaneously, the area of the basin next to it on the left starts to increase at a similar rate, showing the movement of the escape orbits in that direction.

4 Conclusions

In this study, we have explored the effects of different choices for opening Hamiltonian systems, specifically using the Revtokamap as a model due to its representation of magnetic field lines in toroidally confined plasmas, where understanding the escape mechanisms is of interest. The use of linear interpolation to determine exit points allowed for better classification of the basins and revealed the movement and mixing of escape orbits.

By altering the escape configuration in three different cases, we were able to observe both quantitatively and qualitatively the impact of each escape choice. By comparing the colors of the escape basins, a preference for escape through a specific region along the symmetry axis became evident. This was further confirmed by analyzing the distribution of escape areas, as well as the basin entropy and basin boundary entropy in each case.

The most intuitive method of splitting the phase space without considering the dynamic properties led to discontinuities in basin entropy measures at specific perturbation values. This has highlighted the importance of considering the underlying dynamics when designing escape regions.

The movement of the escaping orbits causes issues at the intersection between the exits, creating a transition in the basin boundary that is less smooth than expected. Consequently,

the mixing of the basins increases suddenly when they cross, leading to abrupt changes in both the basin entropy and the basin boundary entropy.

When the exits were rotated, most of the uncertainty was suppressed until higher values of perturbation K , showing a better configuration for reinforcement in a real machine.

Furthermore, by expanding the number of exits, we observed a more detailed and accurate representation of the escape basins, and confirmed the preference for a certain escape region.

Acknowledgments

This work has been supported by grants from the Brazilian Government Agencies CNPq and CAPES. P. Haerter received partial financial support from the following Brazilian government agencies: CNPq (140920/2022-6), CAPES (88887.898818/2023-00). R. L. Viana received partial financial support from the following Brazilian government agencies: CNPq (403120/2021-7, 301019/2019-3), CAPES (88881.143103/2017-01). Finally, M.A.F. Sanjuan acknowledges financial support by the Spanish State Research Agency (AEI) and the European Regional Development Fund (ERDF, EU) under Project No. PID2023-148160NB-I00.

References

- [1] H. E. Nusse, J. A. Yorke, “Basins of Attraction” *Science* 271, 1376–1380 (1996).
- [2] J. Aguirre, R. L. Viana, M. A. F. Sanjuán, “Fractal structures in nonlinear dynamics” *Rev. Mod. Phys.* 81, 333–386 (2009).
- [3] A. Daza, A. Wagemakers, B. Georgeot, D. Guéry-Odelin, M. A. F. Sanjuán, “Basin entropy: a new tool to analyze uncertainty in dynamical systems” *Scientific Reports* 6, 31416 (2016).
- [4] M. A. F. Sanjuán, T. Horita, K. Aihara, “Opening a closed Hamiltonian map” *Chaos* 13, 17–24 (2003).
- [5] J. Schneider, T. Tél, Z. Neufeld, “Dynamics of “leaking” Hamiltonian systems” *Phys. Rev. E* 66, 066218 (2002).
- [6] J. Aguirre, J. C. Vallejo, M. A. F. Sanjuán, “Wada basins and chaotic invariant sets in the Hénon-Heiles system” *Phys. Rev. E* 64, 066208 (2001).
- [7] R. Balescu, “Hamiltonian nontwist map for magnetic field lines with locally reversed shear in toroidal geometry” *Phys. Rev. E* 58, 3781–3792 (1998).
- [8] A. C. Mathias, G. Perotto, R. L. Viana, A. Schelin, I. L. Caldas, “Fractal Structures and Magnetic Footprints in a Divertor Tokamak” *IJBC* 32, 2250078 (2022).
- [9] P. Haerter, L. C. de Souza, A. C. Mathias, R. L. Viana, I. L. Caldas, “Basin Entropy and Wada Property of Magnetic Field Line Escape in Toroidal Plasmas with Reversed Shear” *IJBC* 33, 2330022 (2023).
- [10] R. Balescu, M. Vlad, F. Spineanu, “Tokamak: A Hamiltonian twist map for magnetic field lines in a toroidal geometry” *Phys. Rev. E* 58, 951–964 (1998).

- [11] L. C. Souza, A. C. Mathias, P. Haerter, R. L. Viana, “Basin Entropy and Shearless Barrier Breakup in Open Non-Twist Hamiltonian Systems” *Entropy* 25, 1142 (2023)
- [12] R. L. Viana, I. L. Caldas, J. D. Szezech Jr., A. M. Batista, C. V. Abud, A. B. Schelin, M. Mugnaine, M. S. Santos, B. B. Leal, B. Bartoloni, A. C. Mathias, J. V. Gomes, P. J. Morrison, “Transport Barriers in Symplectic Maps” *Brazilian Journal of Physics* 51, 899–909 (2021).